Supplementary information

Recurrent loss of heterozygosity in 1p36 associated with *TNFRSF14* mutations in *IRF4* translocation negative pediatric follicular lymphomas

Idoia Martin-Guerrero,[1,2*] Itziar Salaverria,[1*] Birgit Burkhardt,[3,4] Monika Szczepanowski,[5] Michael Baudis,[6] Susanne Bens,[1] Laurence de Leval,[7] Africa Garcia-Orad,[2] Heike Horn,[8] Jasmin Lisfeld,[3] Shoji Pellissery,[1] Wolfram Klapper,[5] Ilske Oschlies,[5] and Reiner Siebert[1]

[1]Institute of Human Genetics, University Hospital Schleswig-Holstein Campus Kiel/Christian-Albrechts University Kiel, Kiel, Germany; [2]Department of Genetics, Physical Anthropology and Animal Physiology, University of the Basque Country, UPV-EHU, Spain; [3]NHL-BFM Study Center, Department of Pediatric Hematology and Oncology, Justus-Liebig-University, Giessen, Germany; [4]Pediatric Hematology and Oncology, University Hospital Münster, Germany; [5]Department of Pathology, Hematopathology Section and Lymph Node Registry, Christian-Albrechts University, Kiel, Germany; [6]Institute of Molecular Life Sciences, University of Zurich, Zurich, Switzerland & Swiss Institute of Bioinformatics, University of Zurich, Zurich, Switzerland [7]Institute of Pathology, CHUV, University Hospital of Lausanne, Switzerland; [8]Department of Clinical Pathology, Robert-Bosch-Hospital and Dr. Margarete Fischer-Bosch-Institute of Clinical Pharmacology Stuttgart, Germany

I. Methods

Determination of tumor content

The tumor cell content was estimated by visual inspection on full slides of the respective lymphoma block used for the molecular analyses with help of the immunohistochemical stains for CD20 and at least one T-cell marker. Confusion with reactive B-cell-areas should not have caused significant wrong estimations as usually the lymphoma was more or less completely effacing the preexisting B-cell areas and as significant areas with small reactive follicles can be recognized cytologically even within the CD20-staining.

The OncoScan FFPE Express assay copy number and somatic mutation determination

DNAs from formalin-fixed paraffin-embedded material were hybridized on the MIP-assay using Oncoscan FFPE Express custom service (Affymetrix, Santa Clara, USA). Copy number determination of MIP-assay has been previously described.[1] Briefly, MIP probes are oligonucleotides in which the two end sequences are complementary to two adjacent genomic sequences; these two ends anneal to the genomic DNA in an inverted fashion with a single base between them (generally the site of a single nucleotide polymorphism; SNP). In copy number analysis, genomic DNA is hybridized to the MIP probe and the reaction split into two separate tubes containing paired nucleotide mixes.[2] Amplification and ligation allows circularization of the MIP probe. The probes are then amplified, labeled, detected and quantified by hybridization to tag microarrays. Gains and losses were defined by the use of a trial version of Nexus 6.0 beta Discovery Edition (Biodiscovery, El Segundo, USA) that integrates the genomic identification of significant targets in Cancer (GISTIC) algorithm for identifying significant regions of common genomic aberrations as well as the Allele specific Copy number Analysis of tumors (ASCAT) algorithm for addressing sample aneuploidy and mosaicism. The average resolution was of ~9 Kb/probe for whole genome backbone and ~3 Kb/probe for intragenic regions.

OncoScan FFPE Express also analyzes ~300 somatic mutations in relevant cancer genes. These files are generated from the raw CEL files as part of the primary data analysis process using Affymetrix software. Each sample has a score for each assay (each assay interrogates one previously described mutation). According to manufacturer's instructions a score of 9 or higher indicates that an assay is a valid somatic mutation for that sample. According to this criterion, PIK3CA_pR88Q_c263G_A, FBXW7_pR278X_c832C_T, ABL1_pF359V_c1075T_G, NOTCH1_pL1586P_c4757T_C, PTEN_p_c165_minus_2A_C and PTEN_pQ110X_c328C_T mutations were found. No mutation detected by MIP assay was confirmed by Sanger sequencing.

Array-CGH

Microarray analysis has been performed using the Human Genome CGH Microarray 244A platform (Agilent Technologies, Santa Clara, USA). Experimental procedures were performed according to the manufacturer's instructions. The array was scanned with the DNA microarray scanner (Agilent Technologies) at a resolution of 5µm/pixel. Signal intensities from the generated images were measured and evaluated with the Feature Extraction v10.7.3.1 and Agilent Genomic Workbench Standard Edition 6.5.0.58 software packages (Agilent Technologies). The average genome-wide resolution was of 0.65 Mb.

Mutations

Non-synonymous mutations were tested for their functional consequences *in silico* by using different aminoacid substitution prediction algorithms, including SIFT (Sorting Intolerant From Tolerant) and PolyPhen-2 (Polymorphism Phenotyping).

Statistical analyses

Statistical analyses were performed using PASW Statistics software version 18 (SPSS Inc., Chicago, USA). Chi-Square or Fisher´s exact tests were used to determine the significance of any differences between the clinical variables in samples with genomic aberrations *vs.* wild

type. Overall survival (OS) was defined as the time from diagnosis to date of most recent follow-up. All statistical tests were considered significant at $P \leq 0.05$.

Informed consent

The study was performed in the framework of the BFM-NHL trial, for which central and local institutional review board approvals were obtained and according to the guidelines of the MMML Network Project of the Deutsche Krebshilfe (approved by the IRB of the Medical Faculty Kiel under 403/05).

I. Supplementary tables

Supplementary Table S1. Clinical, pathological and FISH data in pediatric FL

ID	Diag	2nd lymphoma component (%)	Age, sex	Tumor cells %	Stage	Loc	BCL2 exp^	Remnants of reactive B-follicles	Marginal zone diff	Treatment Protocol	Outcome	Follow-up (m)	*BCL2/ t(14;18)*	*BCL6*	*MYC*	*IRF4*	*IGH*	*Ref Oschlies et al*[3]
pFL1	FL3a	-	8,m	70	II	LN (c)	no	yes	yes	NHL-BFM 90	LFU in CR	114	wt	wt	na	wt	wt	4
pFL2	FL3a	FL 1	11,m	65	I	LN (c)	no	yes	yes	NHL-BFM 90	LFU in CR	84	wt	wt	wt	wt	wt	6
pFL3	FL3b	DLBCL (90) [&]	15,m	65	III	LN (ab), intestine	yes (partial)	yes	no	NHL-BFM 95	LFU in CR	156	wt	wt	na	na	split	10
pFL4	FL3b	DLBCL (50)[$]	8,m	90	II	T, LN (c)	yes	yes	no	NHL-BFM 90	LFU in CR	120	wt	wt	wt	na	split	13
pFL5	FL3b	-	10,f	95	III	LN (c, ax, med, ab, ing)	yes	no	no	NHL-BFM 95	Relapse DD second malignancy**	112	wt	split	wt	wt[#]	split	16
pFL6	FL3a	FL 2	16,m	90	I	LN (c)	yes	no	no	NHL-BFM 95	LFU in CR	17	wt	wt	wt	wt	na	18
pFL7	FL3a	-	17,m	80	I	LN (c)	yes (partial)	no	yes	B-NHL BFM 04	Alive in CR	59	wt	wt	wt	wt	wt	21
pFL8[†]	FL3b	DLBCL (30)	6,f	75	II	LN (c)	no	no	no	Ritux + B-NHL BFM 04	Alive in CR	24	wt	wt	wt	wt	wt	23
pFL9	FL3a	FL2	15,f	75	I	LN (c)	yes	yes	no	B-NHL BFM 04	Alive in CR	24	wt	wt	wt	wt	wt	25
pFL10	FL3a	-	6,m	70	na	LN (femoral)	yes	na	yes	R-CHOP	LFU in CR	36	wt	wt	wt	wt[#]	wt	-
pFL11	FL3a	-	10,m	75	II	LN (c)	yes (weak)	yes	yes	B-NHL BFM 04	Alive in CR	19	wt	wt	wt	wt	wt	-
pFL12	FL2	-	17,f	80	na	LN (c, med)	yes	no	no	na	na	na	na	na	na	na	na	-
pFL13	FL3b	-	6,f	20	I	LN (retroauricular)	yes	yes (majority)	no	complete extirpation, w&w	Alive in CR	11	wt	wt	wt	wt	wt	-
pFL14	FL3a	FL1 and 2	18,m	80	I	LN (ing)	yes	yes	no	complete extirpation, w&w	Alive in CR	16	wt	wt	wt	wt	wt	-
pFL15	FL3a	DLBCL (15)	9,f	90	III	T, LN (c,ax,ab), liver, intestine	yes	yes (in tonsil)	no	NHL-BFM 95	LFU in CR	102	wt	wt	wt	wt	split	5
pFL16	FL3b	-	18,f	65	II	LN (ing)	na	no	no	Ritux	LFU in CR	39	wt	wt	wt	wt[#]	wt	-
pFL17	FL3*	-	9,m	50	na	LN (c)	na	yes	no	na	na	na	wt	wt	wt	wt	na	-
pFL18	FL2	-	18,m	80	I	LN (c)	na	no	no	complete extirpation, w&w	Alive in CR	36	wt	wt	wt	wt	wt	-

Abbreviations: Diag, diagnosis; Loc, localization; FL, follicular lymphoma; DLBCL, diffuse large B-cell lymphoma; m, male; f, female; LN, lymph nodes; diff, differentiation; DD, differential diagnosis; T, tonsil; c, cervical including nuchal and submental; ing, inguinal; med, mediastinal; ax, axillary; ab, abdominal; wt, wild type; na, not available; FU, follow-up; LFU, lost to follow-up; CR, complete remission; w&w, watch and wait; m, month; Ref, reference

* Diagnosis as FL3a or FL3b was not available; [#] Multiple *IRF4* copies were detected by FISH; [†] The case pFL8 presents starry sky pattern- Burkitt like pattern; ** Nijmegen-breakage syndrome; differentiation between relapse and second malignancy not possible (no molecular genetics); another relapse DD second malignancy (no molecular genetics) 8 years after first lymphoma; alive; [&] The case pFL3 shows the diffuse growth in 90% of the biopsy as this is an infiltration of the intestinal wall. A secondary colonization of preexisting follicles of the Payer Plaques cannot be ruled out. Nevertheless, the histopathology nor an additional staining for FDC-networks does not allow to differentiate in this case between secondary involvement and focal true follicular growth. [$] The architecture and extension of the follicular component did not resemble secondary colonization of preexisting follicles; ^BCL2 expression data of ten cases were previously published by Oschlies et al, 2010[3]

Supplementary Table S2. Primer information for mutational analyses.

Gene	Primer	Nucleotide sequence (5´-3´)	PCR product (bp)
TNFRSF14	TNFRSF14_ex1_F	TCCTCTGCTGGAGTTCATCC	209
	TNFRSF14_ex1_R	CATGGGGAAGAGATCTGTGG	
	TNFRSF14_ex2_F	ATCTCCCAATGCCTGTCCT	202
	TNFRSF14_ex2_R	AGAAGGGGGCAAGAGTGTCT	
	TNFRSF14_ex3_F	TAGCTGGTGTCTCCCTGCTT	250
	TNFRSF14_ex3_R	GGCTGTGCTGGCCTCTTAC	
	TNFRSF14_ex4_F	TCCACGTACCCCTCTCAGC	228
	TNFRSF14_ex4_R	GAAATGGGAGGGGTGTCC	
	TNFRSF14_ex5_F	CCTCTGTCCGTCCCTCTCTT	218
	TNFRSF14_ex5_R	ACCTTCAAGCCTTTCTGCTG	
	TNFRSF14_ex6_F	CTCCCTGAGGCTGAGTGAAC	277
	TNFRSF14_ex6_R	GGTGACAGAGCTCCAAGAGG	
	TNFRSF14_ex7_F	CTGTGTCCCCTGATCAGACA	204
	TNFRSF14_ex7_R	CAGGACCCTCAGAGAACTGG	
	TNFRSF14_ex8_F	AAAATGAACCCGAGAACCTG	267
	TNFRSF14_ex8_R	AGGTGGACAGCCTCTTTCAG	
ABL1	ABL1_F359V_F	GCTGTACATGGCCACTCAGAT	224
	ABL1_F359V_R	GAGCCTAGTGTTTGCCTTTGTT	
NOTCH1	NOTCH1_L1586P_F	ACCAGTACTGCAAGGACCACTT	220
	NOTCH1_L1586P_R	AAGACCACGTTGGTGTGCAG	
STK11	STK11_Q170X_F	CCGCAGGTACTTCTGTCAGC	128
	STK11_Q170X_R	CCAGGTCGGAGATTTTGAGG	
PIK3CA	PIK3CA_R88Q_F	GCCTCCGTGAGGCTACATTA	233
	PIK3CA_R88Q_R	GAGGATCTTTTCTTCACGGTTG	
FBXW7	FBXW7_R278X_F	ATAGAGCTGGAGTGGACCAGAG	212
	FBXW7_R278X_R	TGTTTAAAGGTGGTAGCTGTTGAG	
PTEN	PTEN_p_c165_F	AAATCTGTCTTTTGGTTTTTCTTG	274
	PTEN_p_c165_R	AATCGGTTTAGGAATACAATTCTG	
	PTEN_pQ110X_F	TAACCCACCACAGCTAGAACTT	289
	PTEN_pQ110X_R	GAAACCCAAAATCTGTTTTCCA	

Supplementary Table S3. Genetic alterations of pediatric follicular lymphomas.

ID	No. CN alt/ CNN-LOH	CN gains	CN losses	CNN-LOH	*TNFRSF14* status	*EZH2* status	Reference Oschlies et al.[3]
pFL1	0	no	no	na	wt	wt	4
pFL2	0	no	no	na	wt	wt	6
pFL3	na	na	na	na	P16S	c.1922 A>T	10
pFL4	7	11q22.1-q25, 17q25.1-q25.3, Xpter-q28	4, 6q11.1-qter, 17p13.3-q11.1, Xq28-qter	no	T272I/G232S	wt	13
pFL5	20	1q21.1-q41, 2p16.2-p12, 3pter-p14.2, 3q13.11-q13.32, **6pter-p22.1,** 13q21.1-qter, 18q12.3-qter, 19q13.31-qter, Xq21.1-q22.2, Xq26.3-qter	1pter-p12, 2q12.1-q22.3, 2q35-qter, 3q13.32-q24, 6q11.1-qter,10p12.1-p11.1, 10q24.32-qter,12q23.1-qter, 13q11-q21.1, 18pter-q11.1	no	wt	wt	16
pFL6	0	no	no	no	wt	wt	18
pFL7	1	no	no	1p36.2-p34.1	S14C/ g.370T>C	wt	21
pFL8	5	10, 11q12.1-q23.3, **11q23.3**	11q23.3-q25	17q12-q21.2	wt	wt	23
pFL9	0	no	no	no	wt	wt	25
pFL10	3	**6pter-p22.3**, 7q31.1-q36.3	no	1pter-p36.13	g.370T>A	wt	-
pFL11	0	no	no	no	wt	wt	-
pFL12	1	7	no	na	P9T	wt	-
pFL13	0	no	no	no	wt	wt	-
pFL14	1	no	no	1pter-p36.13	Q180X	wt	-
pFL15	na	nd	nd	na	nd	c.1922 A>T	5
pFL16	1	6pter-p24.3	no	na	wt	wt	-
pFL17	0	no	no	na	V267M	wt	-
pFL18	0	no	no	na	wt	wt	-

Abbreviations: CN alt, copy number alterations; CNN-LOH, copy number neutral loss of heterozygosity; nd, not done; na, not available; wt, wild type
Notes: Regions in bold correspond to copy number gains of more than two copies /amplifications.
The table does not include "silent" mutations or polymorphisms.

Supplementary Table S4. Whole copy number data of pediatric follicular lymphomas.

Case	CN status	chr	start	end	Size (Mb)
ONCOSCAN					
pFL1					
	no aberrations				
pFL2					
	no aberrations				
pFL4					
	High Gain	**11q22.1-q25**	99,634,634	134,324,142	34,69
	Gain	17q25.1-q25.3	69,229,399	78,723,423	9,49
	Gain	Xpter-q28	0	146,983,016	146,93
	Loss	Xq28-qter	146,983,017-	154,664,758	7,68
	Loss	4	0	191,273,063	191,27
	Loss	6q11.1-qter	61,941,918-	170,899,992	108,96
	Loss	17pter-q11.1	0	22,221,149	22,22
pFL5					
	High Gain	**1q21.1-q41**	143,599,182	215,218,824	71,62
	Gain	2p16.2-p12	53,021,912	76,446,518	23,42
	Gain	3pter-p14.2	0	61,085,250	61,09
	Gain	3q13.11-q13.32	105,664,486	119,311,190	13,65
	Gain	6pter-p22.1	0	29,392,572	29,39
	Gain	13q21.1-qter	54,580,422	114,068,620	59,49
	Gain	18q12.3-qter	40,314,818	76,117,153	35,80
	Gain	19q13.31-qter	49,926,901	63,728,509	13,80
	Gain	Xq21.1-q22.2	81,184,537	102,751,070	21,57
	Gain	Xq26.3-qter	136,020,499	154,913,754	18,89
	Loss	1pter-p12	0	119,845,934	119,85
	Loss	2q12.1-q22.3	104,461,080	145,137,592	40,68
	Loss	2q35-qter	218,893,446	242,634,600	23,74
	Loss	3q13.32-q24	119,441,159	146,084,725	26,64
	Loss	6q11.1-qter	61,871,980	170,821,724	108,95
	Loss	10p12.1-p11.1	24,340,995	38,892,677	14,55
	Loss	10q24.32 - qter	103,978,381	135,198,353	31,22
	Loss	12q23.1 - qter	99,413,038	132,349,534	32,94
	Loss	13q11-q21.1	18,069,540	54,580,422	36,51
	Loss	18pter-q11.1	49,588	16,116,010	16,07
pFL14					
	CNN-LOH	1pter-p36.13	0	18,214,258	18,21
ONCOSCAN/AGILENT244K					
pFL6					
	no alterations				
pFL7					
	CNN-LOH	1p36.32-p34.1	5,151,053	45,818,122	40,67
pFL8					
	Gain	10	0	135,374,737	135,37
	Gain	11q12.1-q23.3	58,686,057	117,196,931	58,51
	High Gain	**11q23.3**	117,207,811	118,931,293	1,72
	Loss	11q23.3-qter	118936,999	134,431,956	15,49
	CNN-LOH	17q21.31 - qter	40,729,078	78,774,742	38,05

pFL09					
	no alterations				
pFL10					
	High Gain	**6pter-p22.3**	0	20,530,644	20,53
	Gain	7q31.1-qter	113,399,531	158,717,957	45,32
	CNN-LOH	1pter-p36.13	0	17,582,810	17,58
pFL11					
	no alterations				
pFL12					
	Gain	7	0	158,821,424	158,82
pFL13					
	no alterations				
AGILENT244K					
pFL16					
	Gain	6pter-p24.3	181,550	9,878,354	9,7
pFL17					
	no alterations				
pFL18					
	no alterations				

Regions in bold correspond to copy number gains of more than two copies/ amplifications

Numbering according to the Human Genome hg18/NCBI build 36.1 assembly

CN: copy number; CNN-LOH, copy number neutral loss of heterozygosity

Supplementary Table S5. *TNFRSF14* mutational analysis of pediatric follicular lymphomas.

Case	Diagnosis	1p36 aberration	Exon	Position[&]	Ref nt	Obs nt	Mutation type	Effect	SIFT prediction (score*)	Polyphen prediction
pFL7	PedFL	yes	1	2486274	C	G	missense	S14C	tolerant (0.05)	benign
			1	2486244	T	C	splice site	-	-	-
pFL10	PedFL	yes	1	2486244	T	A	splice site	-	-	-
pFL14	PedFL	yes	5	2482278	C	T	nonsense	Q180X		
pFL3	PedFL	no	1	2486269	C	T	missense	P16S	tolerant (0.34)	probably damaging
pFL4	PedFL	no	6	2481164	G	A	missense	G232S	tolerant (0.51)	benign
			8	2479743	C	T	missense	T272I	tolerant (0.05)	possibly damaging
pFL12	PedFL	no	1	2486290	C	A	missense	P9T	tolerant (0.6)	benign
pFL17	PedFL	no	8	2479759	G	A	missense	V267M	tolerant (0.14)	benign

PedFL: pediatric follicular lymphoma SIFT: Sorting Intolerant From Tolerant predictor; nt: nucleotide
*Treshold for intolerance is 0.05
[&]Numbering according to the Human Genome hg18/NCBI build 36.1

Supplementary Figures

Supplementary Figure S1. Global series included in the copy number analysis

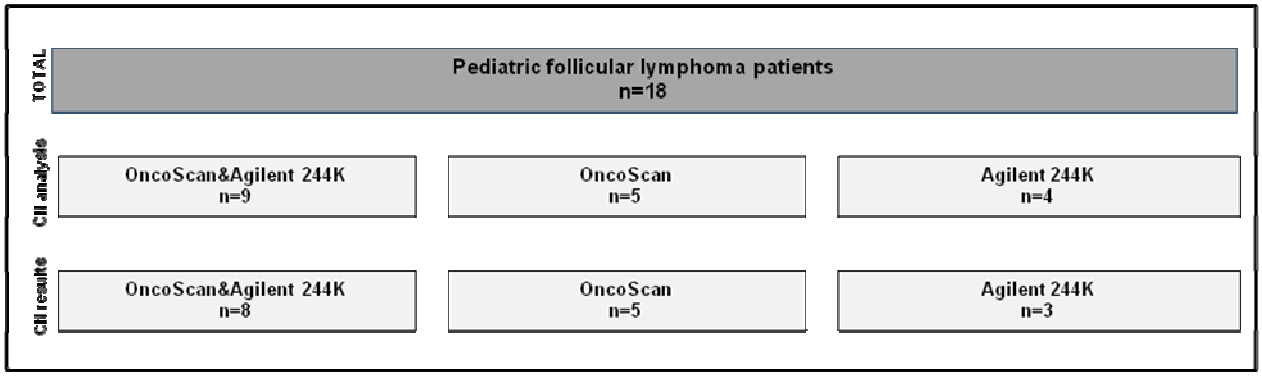

Supplementary Figure S2. (A, B) Gain and amplification of 6p arm detected by MIP-assay in cases pFL5 and pFL10, respectively. A' and B' show FISH validation of the 6p25 gain/amplification, using an *IRF4* break apart probe consisting in PAC-clone RP3-416J7 labeled in orange and BAC-clones RP5-1077H22 and RP5-856G1 labeled in green.

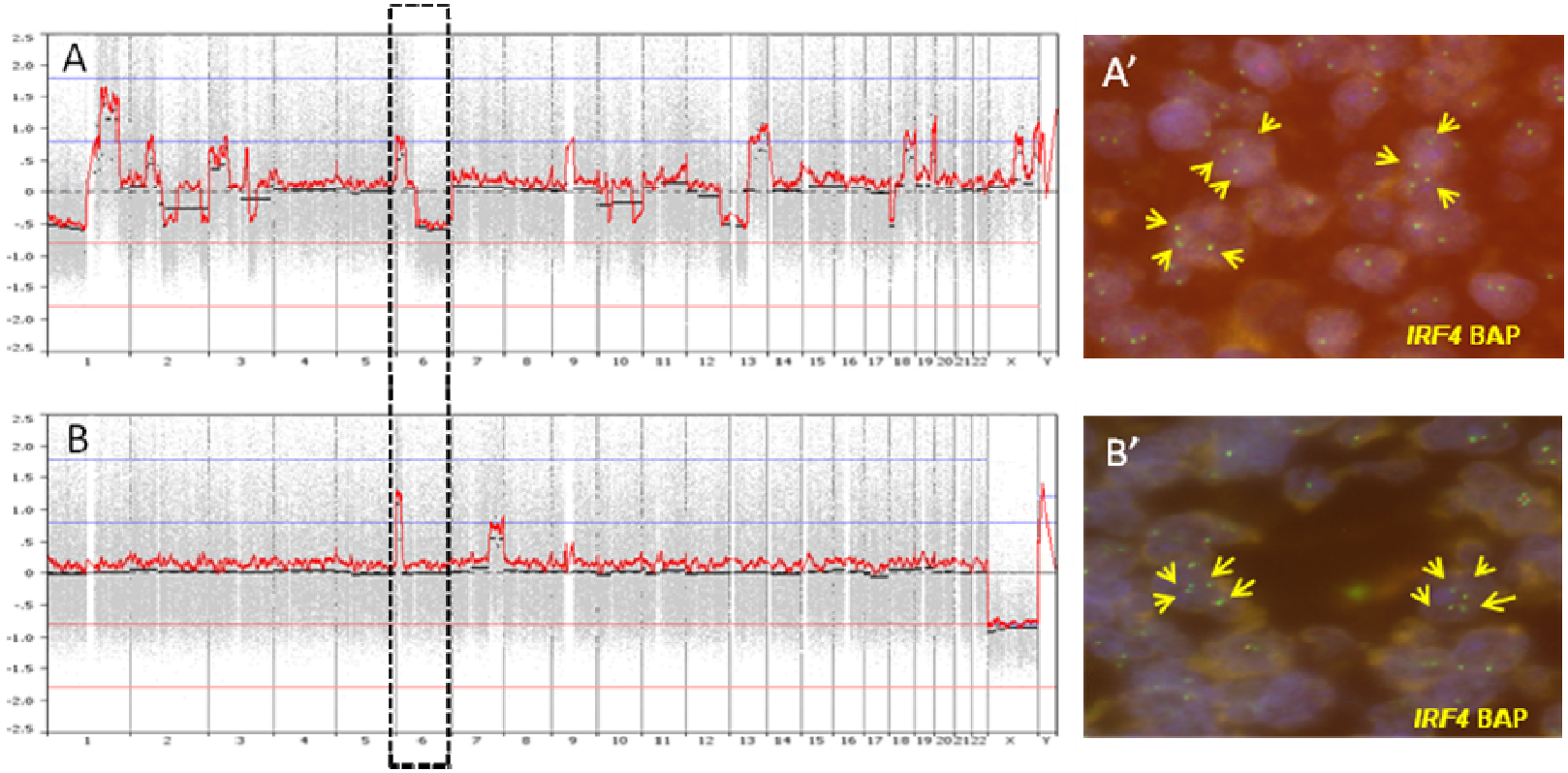

Supplementary Figure S3. Comparison of chromosomal imbalances between pediatric FL and previously published pediatric FL positive for IRF4-translocation.[4]

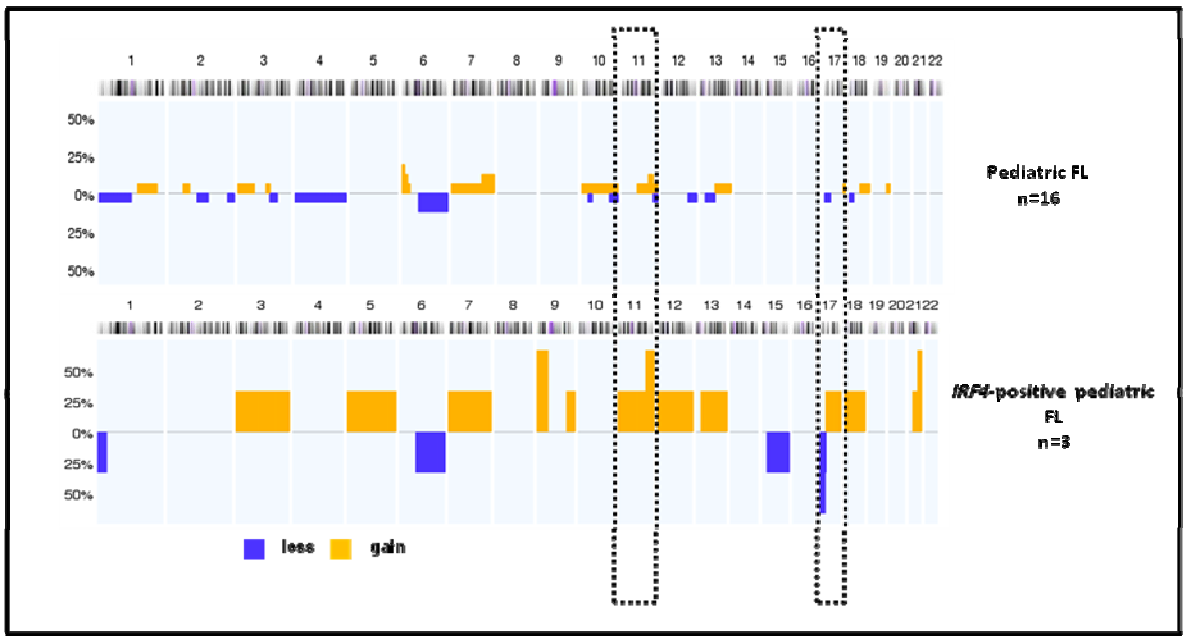

Supplementary references

1. Wang Y, Carlton VE, Karlin-Neumann G, Sapolsky R, Zhang L, Moorhead M, et al. High quality copy number and genotype data from FFPE samples using Molecular Inversion Probe (MIP) microarrays. BMC Med Genomics. 2009;2:8.
2. Wang Y, Moorhead M, Karlin-Neumann G, Wang NJ, Ireland J, Lin S, et al. Analysis of molecular inversion probe performance for allele copy number determination. Genome Biol 2007;8:R246.
3. Oschlies I, Salaverria I, Mahn F, Meinhardt A, Zimmermann M, Woessmann W, et al. Pediatric follicular lymphoma--a clinico-pathological study of a population-based series of patients treated within the Non-Hodgkin's Lymphoma--Berlin-Frankfurt-Munster (NHL-BFM) multicenter trials. Haematologica. 2010;95:253-9.
4. Salaverria I, Martin-Guerrero I, Burkhardt B, Kreuz M, Zenz T, Oschlies I, et al. High Resolution Copy Number Analysis of IRF4 Translocation-positive Diffuse Large B- and Follicular Lymphomas. Genes Chromosomes Cancer. 2013;52(2):150-5.